LARGE SYNOPTIC SURVEY TELESCOPE

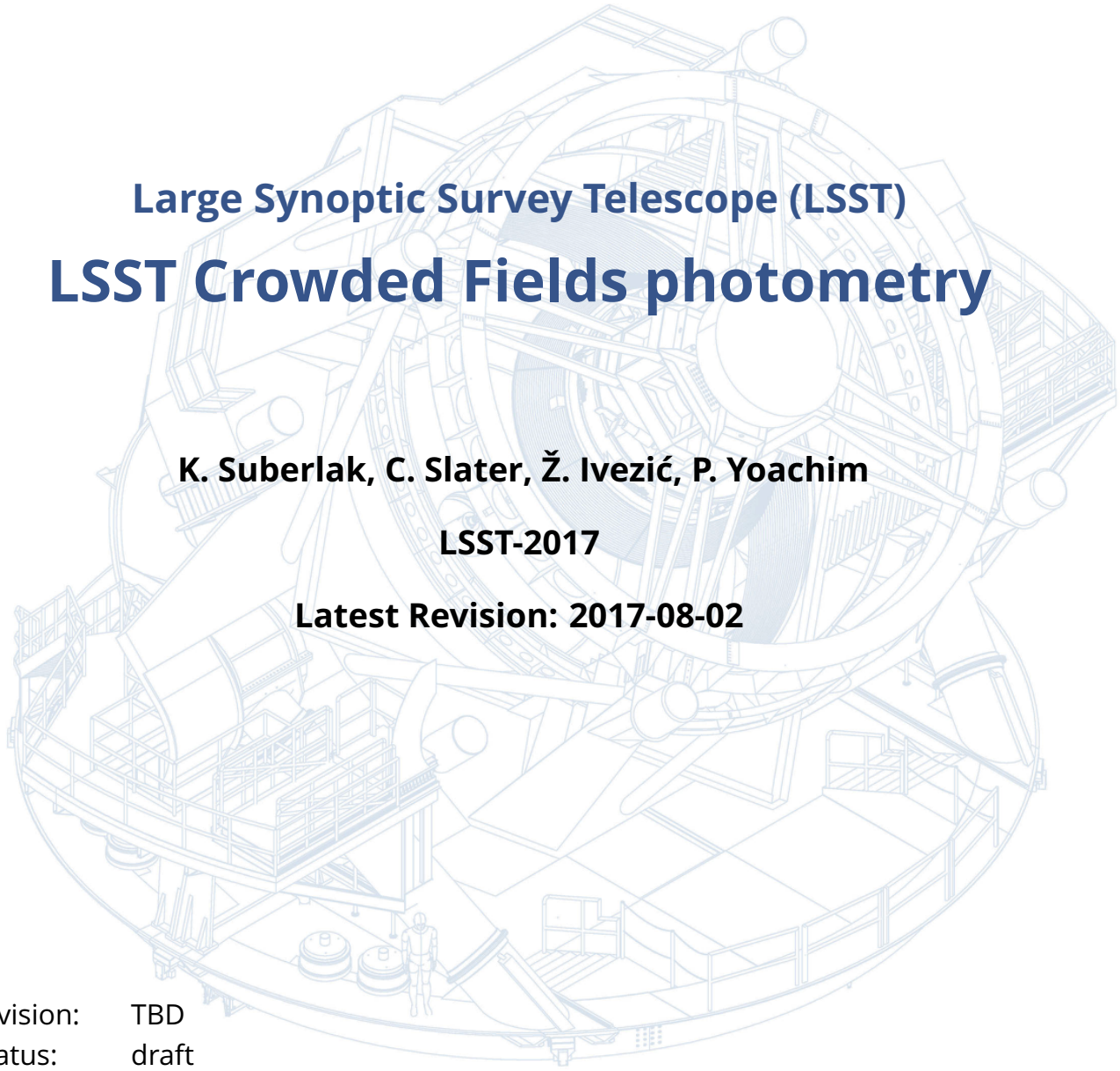

Large Synoptic Survey Telescope (LSST)

LSST Crowded Fields photometry

K. Suberlak, C. Slater, Ž. Ivezić, P. Yoachim

LSST-2017

Latest Revision: 2017-08-02

revision: TBD
status: draft

Abstract

A report the status of crowded field photometry. We evaluate the need for performing better photometry in crowded fields by quantifying areas of the sky at a given density level. We provide an overview of density metrics, photometric methods applicable in a given stellar density regime, and recommendations for areas of improvement in the LSST Stack.

Change Record

Version	Date	Description	Owner name
1	2017-07-16	First draft.	Krzysztof Suberlak

Contents

1 Introduction

This is a document to report on quantifying the performance expectations and options with respect to crowded field processing.

The Large Scale Synoptic Telescope (LSST) will sample very diverse regions when it comes to stellar density, or crowdedness : from high density low-galactic latitude regions that have tens of millions of sources per square degree, to low-density regions towards the galactic poles with less than thousand sources per square degree.

As mentioned by [1] with regards to Hyper Suprime CAM software pipeline (based on LSST Stack, which in turn builds on the experience of the SDSS Photo pipeline), deblending and performing a successful photometry is an inherent part of any astronomical data processing pipeline. The boundaries between deblending, measurement and detection blur in very high stellar densities, and the deeper the survey, the higher the stellar densities that it can encounter (see Sec 4.8.3 in [1]).

The way in which measurements may be affected by the crowdiness have been studied before - pilot study by [2] confirmed the '30 beams per source' rule of thumb, albeit it depends on the source number counts (with steeper number counts we need more beams per source). Following on that exploratory study, [3] describes more quantitative framework to address this issue in the era of large telescopes.

We start with the LSST Metrics Analysis Framework [1] simulated stellar density map [2], made with `sims_maf/python/lsst/sims/maf/maps/createStarDensitymap.py`[3] by Peter Yoachim and Lynne Jones at UW. The dataset `starDensity_r_nside_64.npz` contains 64 magnitude bins, and 49152 healpixels [4]. Each pixel contains information about number of stars per square degree in a given magnitude bin.

Using this data, we select magnitude bins smaller than r=24.5 in the Southern Hemisphere ($\delta < 0$). We add stellar count across magnitude bins (selecting only r <= 24.5 bins). For each pixel we calculate the number of pixels that have a higher stellar count. Since each

[1] `https://www.lsst.org/scientists/simulations/maf`
[2] `https://github.com/lsst/sims_maf`
[3] `https://github.com/lsst/sims_maf/blob/a9bc8f6d00fae5d7ce4ff6ea7279d5a0fca29437/python/lsst/sims/maf/maps/createStarDensitymap.py`
[4] see http://healpix.sourceforge.net for documentation of HEALPix

pixel in HEALPix has an equal area, the fraction of pixel number above a certain threshold corresponds to the fraction of sky area above given density limit. See Fig. 1 for an illustration of how we define the stellar density - it is akin to a cumulative distribution. Therefore 'top 1%' density means that only 1 in 100 pixels has a higher density than a given pixel. Likewise, 'top 10%' means that '10 %' of pixels in the selected hemisphere have higher density.

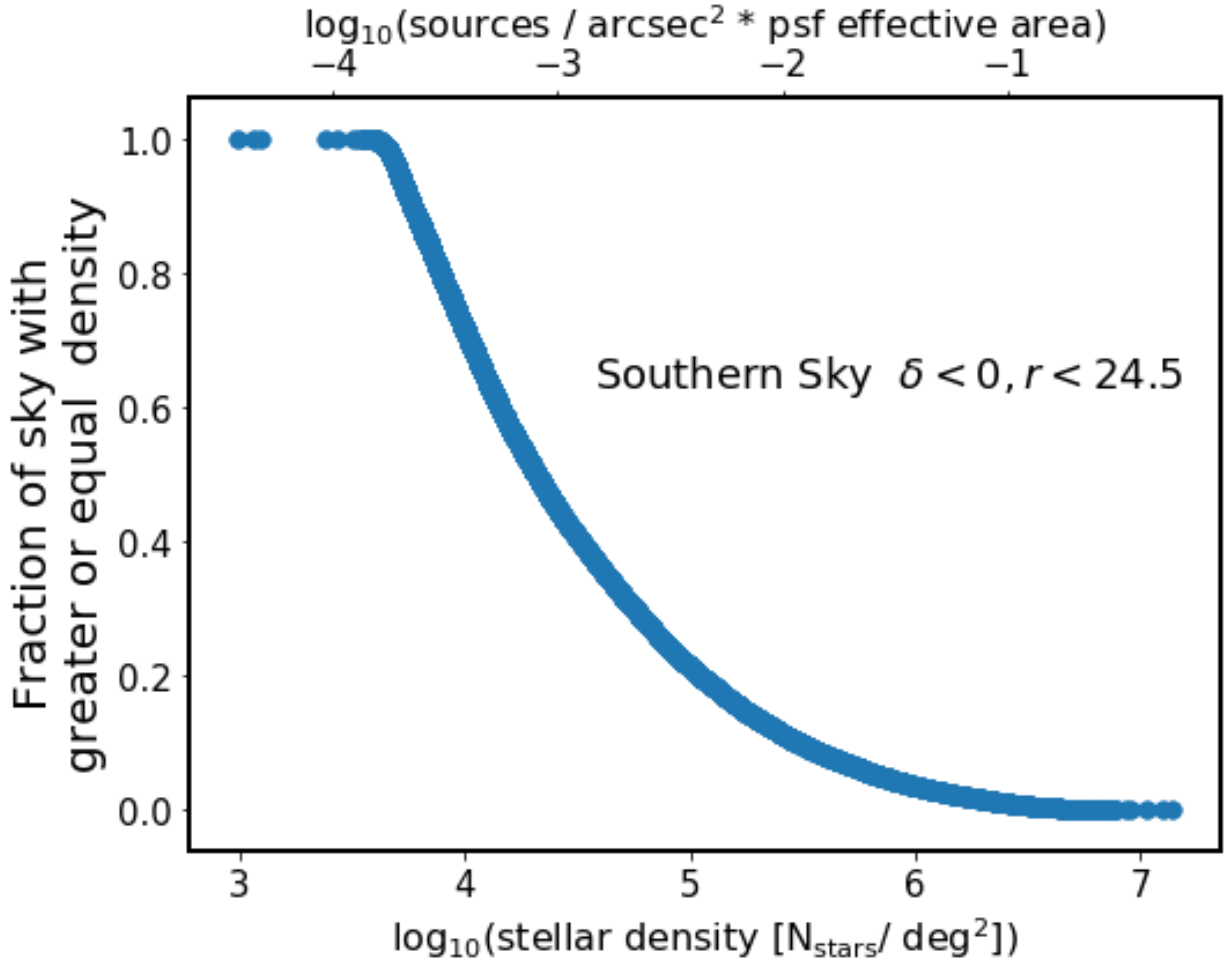

FIGURE 1: Illustration of how the stellar density is quantified in terms of relative pixel density. We express stellar density both in terms of number of stars per square degree (bottom axis), as well as in terms of product of sources per square arcsecond and psf effective area (upper axis)

Since this definition of density includes all pixels that are within 'top 20%', we take selection around the percentiles so that :

- top 1 % means fraction of sky with greater density is 0.01

- 5 % region means such that between 4% and 6%
- 20 % region includes 19% - 21%
- 50 % region includes 49% - 51%

We illustrate the location of pixels representative of these density brackets on the sky in various projections and coordinate systems : cylindrical (Mercator) projection in equatorial coordinates on Fig. 2, Mollweide projection in equatorial coordinates on Fig. 3, and the same in galactic coordinates on Fig. 4.

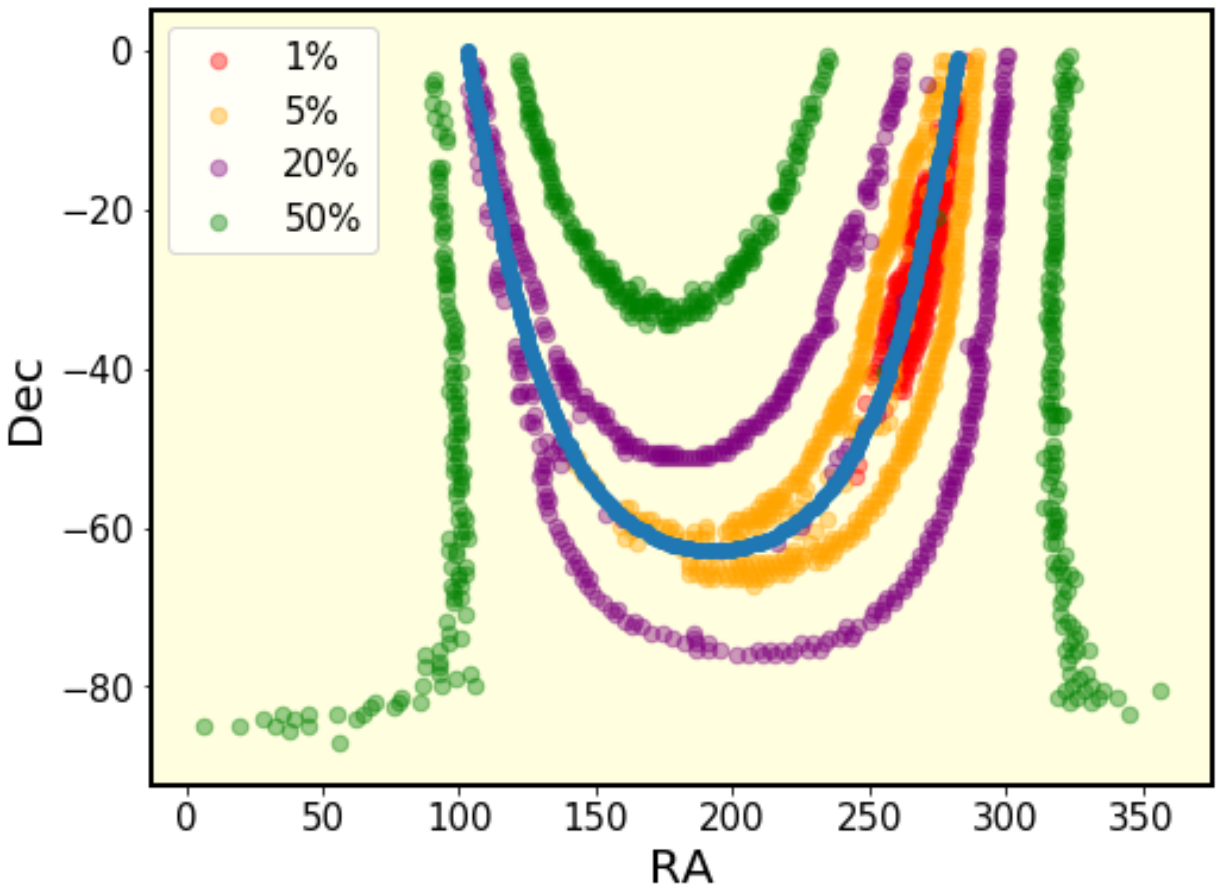

FIGURE 2: Illustration of location of regions representative of different relative density in cylindrical projection, equatorial coordinates. The blue solid line marks the location of Galactic equator.

We compare the MAF estimates of stellar density in different density regimes to Dark Energy Camera (DECam) data, taken with the 4-m Cerro Tololo Inter-American Observatory telescope

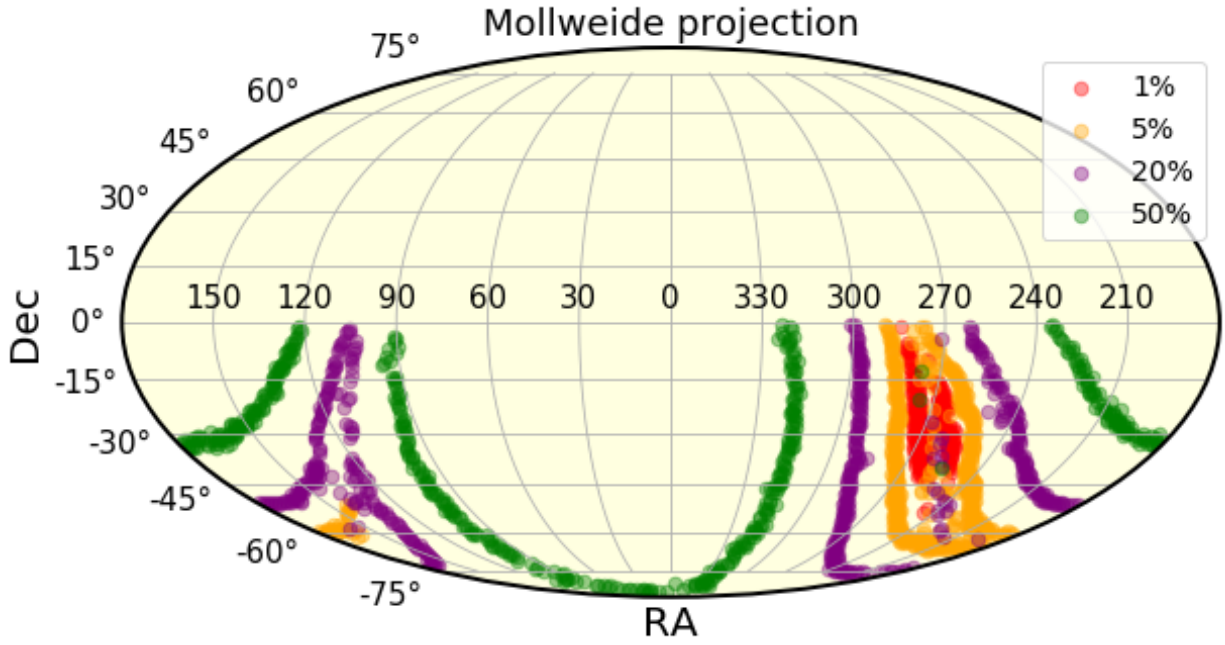

FIGURE 3: Same as Fig. 2, but in Mollweide projection, with Equatorial coordinates.

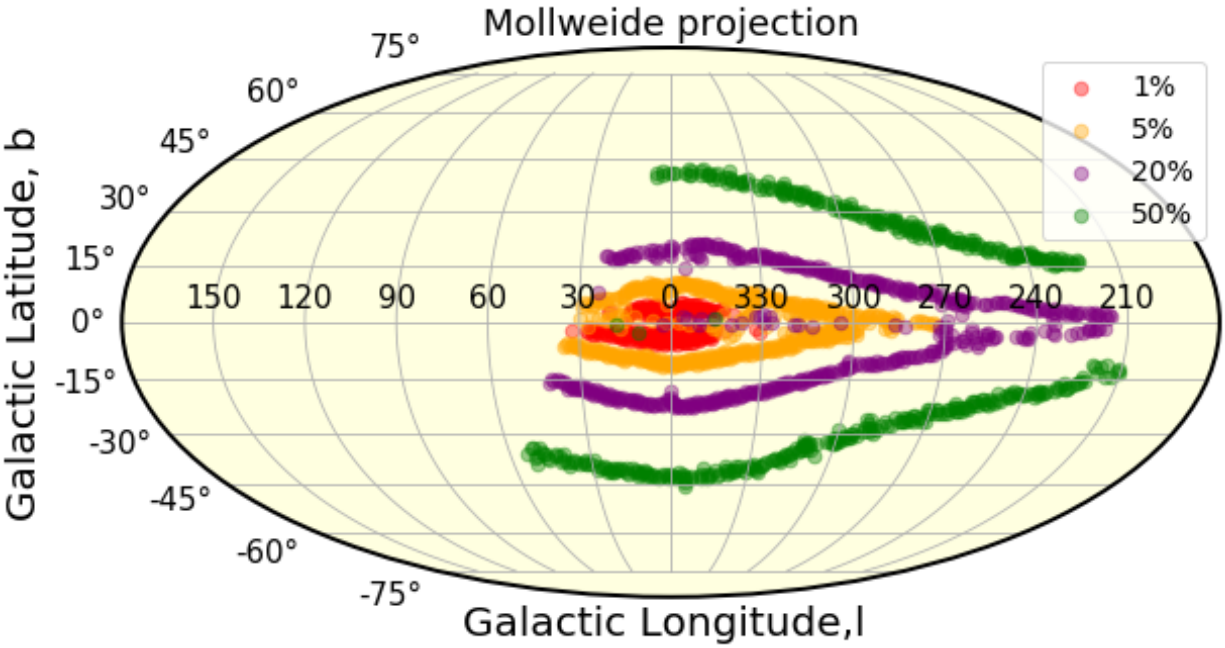

FIGURE 4: Same as Fig. 3, but in Galactic coordinates, which emphasizes the location of regions representing different density with regards to the Milky Way. It makes sense that the highest density regions in the Southern Hemisphere ($\delta < 0$) are located close to the galactic bulge, and the decreasing density regions approximately trace the shape of our galaxy.

(CTIO)[5]. Due to inability of NOAO Data Archive [6] query engine to handle a list of coordinates, we first obtained all data that fulfilled very loose criteria:

- telescope = 'ct4m'
- instrument = 'decam'
- 90 sec < exposure < 125 sec
- release_date < '2017-07-24'
- dec < 0
- proctype = 'InstCal'
- prodtype = 'image'
- filter is u, g, r, or VR

(the SQL query used is available in the Appendix A.1). The exposure was chosen to match the DECam data to the depth that would be achieved by LSST with 30 second exposure.

We obtained 11928 rows fulfilling these criteria : the location of these observations on the sky, with overlaid MAF density regions , is shown on Fig. 5.

We used AstroPy to match the coordinates of MAF healpixels in different density regimes to DECam imaging data. We found that of 244 top 1% density pixels, 91 had DECam matches within 30 arcminutes, as shown on Fig. 6.

Per each density regime, we selected five random DECam fields, and performed source extraction with DAOStarFinder[7]. This tool uses a classic DAOFIND algorithm [4], and we used it to verify the plausibility of the MAF source densities using real data. DECam employs mosaic CCDs - each field, which can be downloaded as a fits.fz compressed file, is split into 60 primary HDUs. FITS viewing software, such as ds9, by default open the first element (HDU[1]), and we decided to perform source extraction on this one element of the mosaic per field, since each

[5] see http://www.ctio.noao.edu/noao/node/1033
[6] http://archive.noao.edu/search/query
[7] http://photutils.readthedocs.io/en/stable/photutils/detection.html

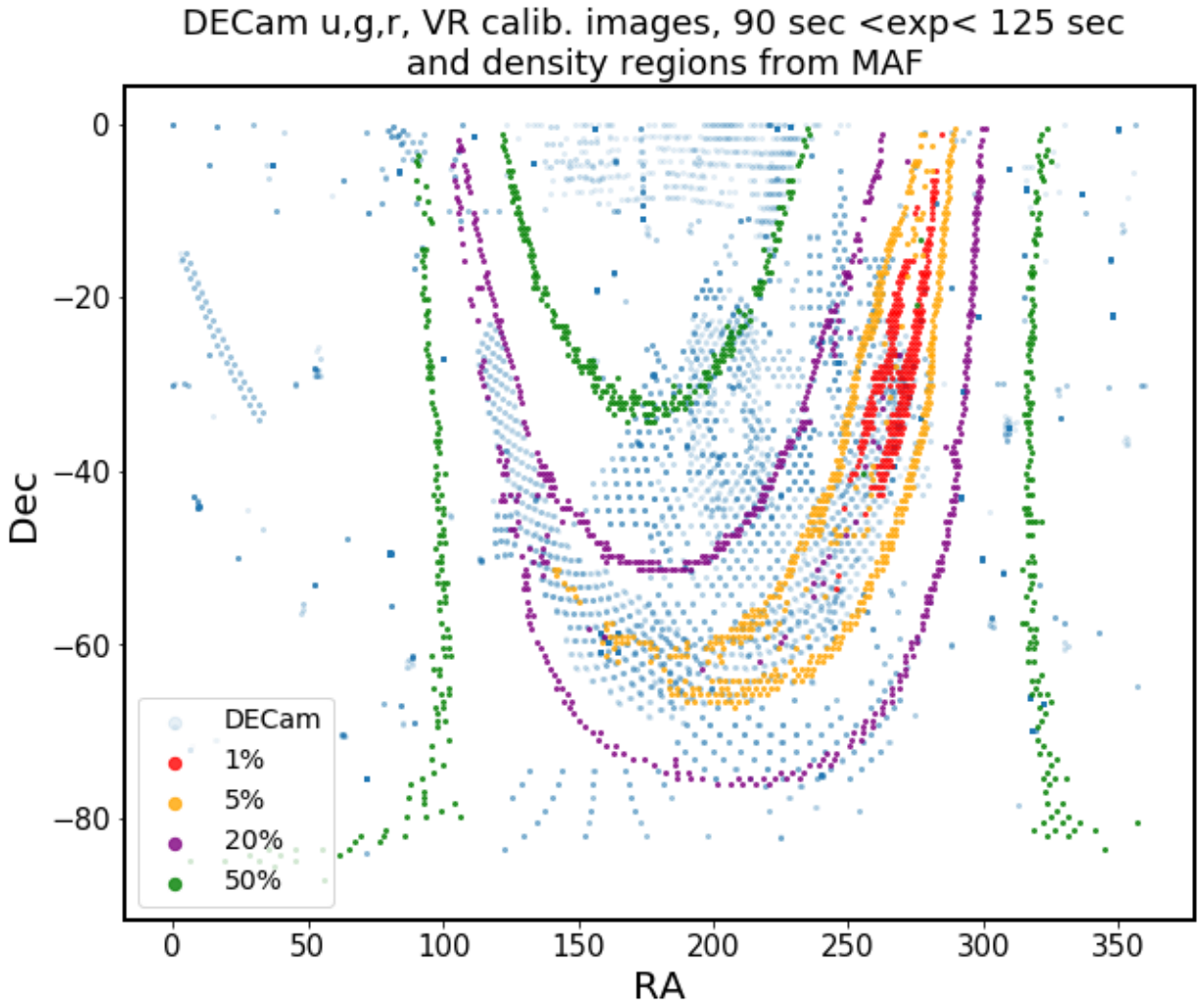

FIGURE 5: DECam observations with exposure $\in [90, 125]$ sec, $\delta < 0$, taken in u,g,r, or VR filter.

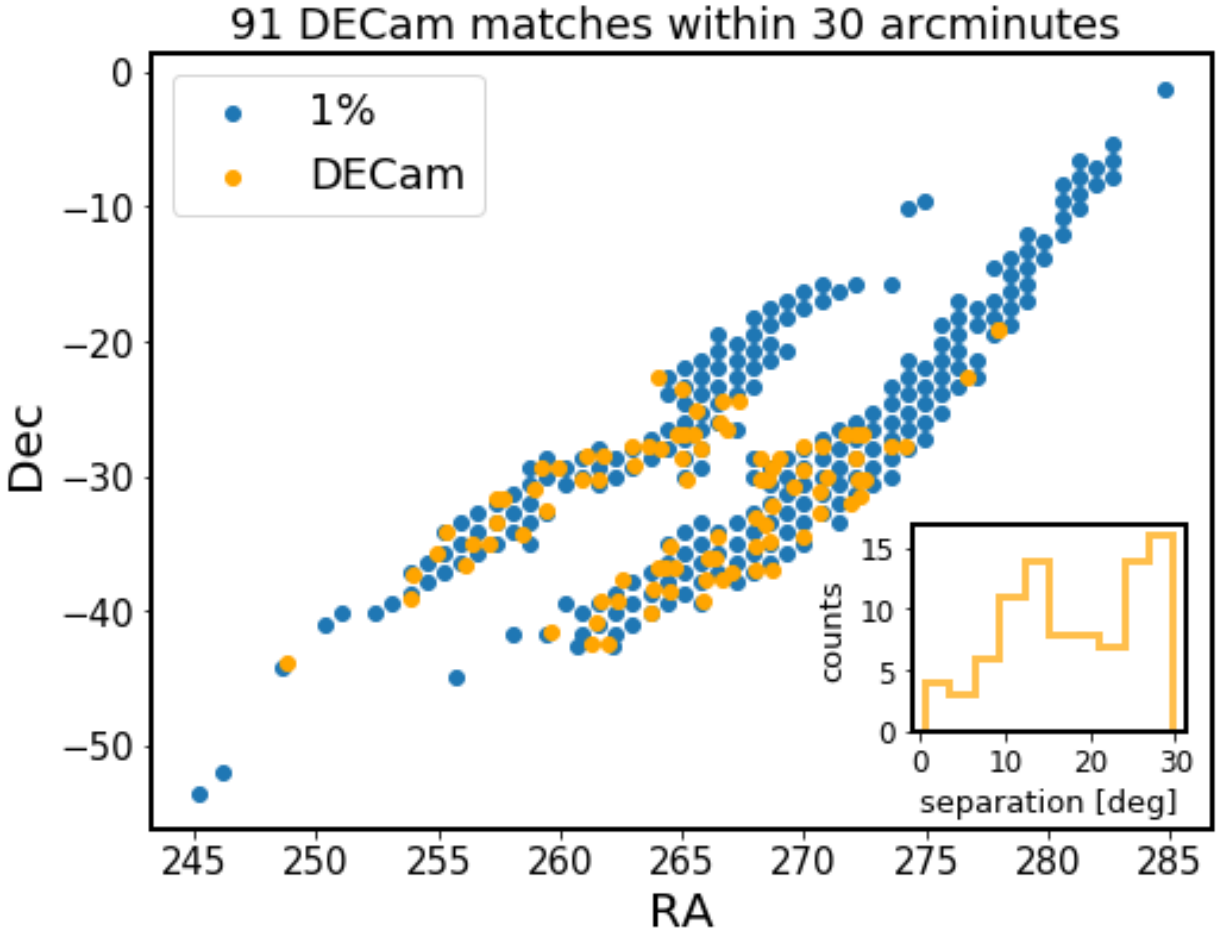

FIGURE 6: DECam observations with exposure $\in [90, 125]$ sec, $\delta < 0$, taken in u,g,r, or VR filter, matched by 2D separation to MAF healpixels within the highest stellar density bins. The inset shows the distribution of separation between healpix coordinates and DECam image center. Each DECam image is a mosaic, and each mosaic element covers approximately 9x18 arcminutes.

archive	ra	dec	TRILEGAL	MAF	DAO
c4d_140624_080728_ooi_r_v1	277.943625	-19.120972	7951830	2650680	498760
c4d_140624_081148_ooi_r_v2	277.981113	-19.083333	7865364	2590488	440755
c4d_170428_094150_ooi_g_v1	268.439875	-33.630111	39882358	4587804	375980
c4d_170504_084722_ooi_g_v1	264.043042	-22.608889	15582905	2833740	561795

TABLE 2: Source density comparison for 1% density level : TRILEGAL, DAO and MAF columns contain stellar counts from TRILEGAL simulation , DAOStarFinder based on DECam data, and MAF simulation, respectively. Simulation results are limited by LSST r < 24.5. All counts are in stars per square degree.

archive	ra	dec	TRILEGAL	MAF	DAO
tu1669764	260.973083	-18.467306	1546620	641484	376915
tu1670143	259.304375	-19.487611	1234484	599508	387454
tu1677011	260.957167	-20.493167	2535014	810144	509093
tu2091292	262.64325	-19.471278	3350692	795996	434409
tu2093190	260.994583	-16.475528	1034980	585576	286712

TABLE 3: Source density comparison for 5% density level, all columns and units as in Table 2

element is of the same size, and is equally representative of the field. The size of each element of the mosaic is 2046x4094 pixels, with pixel scale of 0.27 arcsec / px , so that a single mosaic element covers an area of 0.047117 sq.deg. Using the FWHM information from the FITS header, and sigma clipped standard deviation σ, we performed source extraction with the detection threshold at 5σ level, setting the detection threshold at 5σ, and scaled it up to the source count per square degree to allow comparison with MAF data.

We also obtained TRILEGAL[8] simulation results for each of the DECam fields, submitting to the online form the DECam ra,dec, and field size (using the size of a single mosaic element, as for DAOStarFinder source extraction - approximately 0.047117 sq.deg. per field). We limited the query results selecting r < 24.5 with LSST ugrizy photometric system, keeping all other settings as default. We used the number of sources per TRILEGAL output file, and scaled it to the degree level to compare with MAF and DAO. The results are shown in Tables 2, 5 , **??** , **??** for 1%,5%,20% and 50 % density levels.

A Appendix : SQL queries

A.1 NOAO DECam query

[8] http://stev.oapd.inaf.it/cgi-bin/trilegal

archive	ra	dec	TRILEGAL	MAF	DAO
c4d_160327_041913_ooi_g_v1	239.926333	-24.88225	169132	110160	14814
c4d_170122_055542_ooi_g_v1	120.884	-24.031667	344696	116856	66282
tu1661798	242.794	-23.027278	183671	118188	44216
tu1668579	105.812417	-3.100833	375777	111096	54004
tu2075030	249.378875	-17.461278	210646	109656	41980

TABLE 4: Source density comparison for 20% density level, all columns and units as in Table 2

archive	ra	dec	TRILEGAL	MAF	DAO
c4d_150614_002629_ooi_g_v1	222.213375	-12.759667	28036	20916	7767
c4d_150615_005257_ooi_g_v1	223.138875	-11.249944	26657	21024	12904
c4d_160607_025052_ooi_g_v1	233.175667	-1.679167	27633	20052	13371
c4d_170718_042438_ooi_r_v1	228.030375	-6.490833	27017	20412	17615
tu2046406	91.8075	-14.163028	41344	19944	35974

TABLE 5: Source density comparison for 50% density level, all columns and units as in Table 2

```
SELECT \
  reference, dtpropid, surveyid, release_date, start_date, \
  date_obs, dtpi, ra, dec, telescope, instrument, filter, \
  exposure, obstype, obsmode, proctype, prodtype, seeing, \
  depth, dtacqnam, filesize, md5sum, \
  reference AS archive_file
FROM \
  voi.siap \
WHERE \
  ((exposure > 90) AND (exposure <125 ) )  \
AND release_date < '2017-07-24' \
AND (dec <= 0) \
AND (proctype = 'InstCal') \
AND (prodtype = 'image') \
AND (telescope = 'ct4m') \
AND (instrument = 'decam') \
AND ((filter ILIKE 'u DECam%' ) \
OR (filter ILIKE '%g DECam%' ) \
OR (filter ILIKE '%r DECam%' ) \
OR (filter ILIKE '%VR DECam%' ) ) \
ORDER BY date_obs ASC LIMIT 250000
```

References

[1] Bosch, J., et al. 2017, ArXiv e-prints

[2] Hogg, D. W. 2001, The Astronomical Journal, 121, 1207

[3] Olsen, K. A. G., Blum, R. D., & Rigaut, F. 2003, AJ, 126, 452

[4] Stetson, P. B. 1987, PASP, 99, 191